Mon. Not. R. Astron. Soc. **000**, 000–000 (0000) Printed 2 February 2008 (MN LATEX style file v1.4)

XMM-Newton observations of three short period polars: V347 Pav, GG Leo and EU UMa

Gavin Ramsay[1], Mark Cropper[1], K. O. Mason[1], F. A. Córdova[2], W. Priedhorsky[3]
[1] *Mullard Space Science Laboratory, University College London, Holmbury St. Mary, Dorking, Surrey, RH5 6NT, UK*
[2] *University of California, Riverside, CA 92521, USA*
[3] *Los Alamos National Laboratory, MS D436, Los Alamos, NM 87545, USA*

arXiv:astro-ph/0309110v1 3 Sep 2003

Received:

ABSTRACT

We present phase-resolved *XMM-Newton* data of three short period polars: V347 Pav, GG Leo and EU UMa. All three systems show one dominant accretion region which is seen for approximately half of the orbital cycle. GG Leo shows a strong dip feature in its X-ray and UV light curves which is due to absorption of X-rays from the accretion site by the accretion stream. The emission in the case of EU UMa is dominated by soft X-rays: its soft/hard X-ray ratio is amongst the highest seen in these objects. In contrast, GG Leo and V347 Pav shows a ratio consistent with that predicted by the standard shock model. We infer the mass of the white dwarf and explore the affect of restricting the energy range on the derived parameters.

Key words: Stars: individual: V347 Pav, GG Leo and EU UMa – Stars: binaries – Stars: cataclysmic variables – X-rays: stars

1 INTRODUCTION

Polars or AM Her systems are accreting binary systems in which material transfers from a dwarf secondary star onto a magnetic (B ∼10–200MG) white dwarf through Roche lobe overflow. At some height above the photosphere of the white dwarf a shock forms. Hard X-rays are generated in this post-shock flow. Some of these X-rays are intercepted by the photosphere of the white dwarf and are re-emitted at lower energies. Soft X-rays can also be produced by dense 'blobs' of material which impact directly into the white dwarf. Further, cyclotron emission in the optical band is produced by electrons spiralling around the magnetic field lines (see Warner 1995 for a review).

To better characterise the X-ray emission from polars we have undertaken a survey of 37 systems using *XMM-Newton*. An overview of the survey and initial results are given in Ramsay & Cropper (2003b). We have presented phase-resolved observations of DP Leo, WW Hor (Ramsay et al 2001), BY Cam (Ramsay & Cropper 2002a), CE Gru (Ramsay & Cropper 2002b), EV UMa, RX J1002–1925 and RX J1007–2016 (Ramsay & Cropper 2003a). Here, we present phase-resolved observations on three further polars, V347 Pav (RE J1844–741), GG Leo (RX J1015.6+0904) and EU UMa (RE J1149+28), all of which were discovered using *ROSAT* and have short periods (90, 80 and 90 mins respectively).

2 PRESENT AND PAST OBSERVATIONS

XMM-Newton was launched in Dec 1999 by the European Space Agency. It has the largest effective area of any X-ray satellite and also has a 30 cm optical/UV telescope (the Optical Monitor, OM: Mason et al 2001) allowing simultaneous X-ray and optical/UV coverage. The EPIC instruments contain imaging detectors spanning the energy range 0.1–10keV with moderate spectra resolution. The OM data were taken in two UV filters (UVW1: 2400–3400 Å, UVW2: 1800–2400 Å) and one optical band (V band). The observation log is shown in Table 1. The data obtained using the RGS instruments were of low signal-to-noise and are therefore not discussed further. The data were processed using the *XMM-Newton Science Analysis Software* v5.3.3. For details of the analysis procedure see Ramsay & Cropper (2003a). We show in Table 1 the mean V mag determined using the OM for each source at the time of our observation.

V347 Pav was discovered using the *ROSAT* extreme UV WFC survey (Pounds et al 1993) and identified with a V=16 mag Cataclysmic Variable (CV) by O'Donoghue et al (1993). Bailey et al (1995) confirmed V347 Pav as a polar when large amplitude circular polarisation variations were detected with a period of 90 min. Based on a typical polar X-ray spectrum in the high accretion state, V347 Pav was brighter during the *XMM-Newton* observations compared to March 1993 but not as bright as in July 1994 (Ramsay et al 1996). It was therefore in a high accretion state.

© 0000 RAS

GG Leo was also discovered as part of the *ROSAT* all sky survey, on this occasion using the X-ray Telescope. Followup observations by Burwitz et al (1998) identified the optical counterpart as a $V = 16 - 17$ mag polar with an orbital period close to 90 min. Burwitz et al (1998) reported X-ray data taken from 3 epochs: it was bright on each occasion and showed a narrow dip which was taken to be the accretion stream obscuring the accretion region. Comparing the count rates we find that GG Leo was at a similar X-ray brightness during these *XMM-Newton* observations as in May 1994, so that it was also in a high accretion state.

EU UMa was discovered using the *ROSAT* extreme UV WFC survey and identified with a V=17 mag CV by Mittaz et al (1992). Observations using *EUVE* by Howell et al (1995) found that the orbital period was likely to be 90 mins. X-ray observations using *ROSAT* data (Ramsay et al 1994, Ramsay 1995) showed it had a peak count rate of ∼5 ct/s. We estimate that it was fainter by a factor of 3 in these *XMM-Newton* observations, although it is still likely to have been in a relatively high accretion state.

3 LIGHT CURVES

3.1 V347 Pav

V347 Pav is relatively bright in soft and hard X-rays, peaking at over 1 ct/s (in the EPIC pn detector) in both soft and hard X-ray bands. It shows a distinct faint and bright phase lasting nearly 0.5 cycles each (Figure 1). The count rate in the faint phase is significant at 0.037±0.007 ct/s. The intensity shows a rapid rise at ϕ=0.0 when the bright accretion region comes into view over the limb of the white dwarf. As seen from the hardness ratio curve (Figure 1), the hard X-ray light curve rises more rapidly than the soft X-rays. This is expected since in the standard models (eg Lamb & Masters 1979, King & Lasota 1979) hard X-rays are optically thin whereas the soft X-rays are optically thick. The rapid but not instantaneous rise in the hard X-ray flux indicates that the shock has a significant vertical height above the photosphere of the white dwarf and/or the accretion region is extended. Based on our emission model described in §4.1 we predict that for a white dwarf mass of $1.0M_{\odot}$, a specific accretion rate of 1 g^{-1} s^{-1} cm^{-2} and a magnetic field strength of 20MG (Potter, Cropper & Hakala 2000), the shock height would be ∼0.1 R_{wd}. This is high enough to cause the observed difference in the rise time in the hard X-ray light curve. From the hardness ratio plot, the light curve is harder near the center of the bright phase (ϕ ∼0.35) indicating that some absorption affect maybe present at these phases. The V band data show a rise in flux at the same phase as the onset of the bright phase.

Phase zero on the optical ephemeris of Ramsay et al (1996) was defined as the start of the rapid rise from the faint phase. The accumulated error in that ephemeris is ϕ=0.02. Phasing our data on that ephemeris shows the bright phase starting at a much earlier phase (ϕ=0.8). We revisited the optical data and included the timing of the start of the bright phase reported by Bailey et al (1995). We find that the period of Ramsay et al (1996) was actually a one day alias of the true orbital period. The best fit ephemeris is:

$$T = HJD2448475.2913(5) + 0.062557097(36) \quad (1)$$

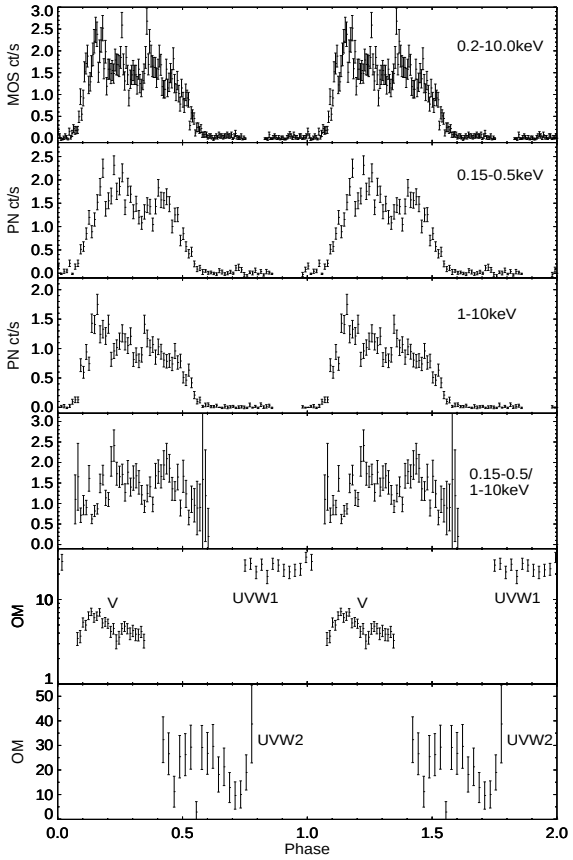

Figure 1. The phased and binned X-ray and optical light curves of V347 Pav. We have folded the data on the ephemeris reported in §3.1. Energy bands 0.15–0.5keV and 1.0–10.0keV have bin widths of 60 sec (=0.011 cycles), while the energy band 0.2-10.0keV has a bin width of 30 sec (=0.0055 cycles). The optical data were binned into 60sec bins, while the UV data was binned into 120 sec bins (=0.022 cycles). The units for the OM data are 10^{-16} ergs s^{-1} cm^{-2}Å^{-1}.

We have therefore used the above ephemeris to phase our data. We also re-analysed the *ROSAT* data shown by Ramsay et al (1996). We find that all those data are consistent with the main accretion region being the prime source of X-rays. The fact that Ramsay et al (1996) found the phase of the bright X-ray region to vary is phase was therefore due to the use of an incorrect ephemeris.

3.2 GG Leo

Like V347 Pav, GG Leo shows a relatively high count rate in both X-ray bands (∼1 ct/s in the EPIC pn detector). It has a faint phase lasting $\Delta\phi \sim 0.3$ cycles and a bright phase lasting $\Delta\phi \sim 0.7$ (Figure 2). This implies the X-ray bright accretion region is located in the upper hemisphere of the white dwarf or is significantly extended. Although faint, the source is again clearly visible during the faint phase (0.050±0.009 ct/s). This soft X-ray light curve is similar to those seen using *ROSAT* data (Burwitz et al 1998). Burwitz et al (1998) also report *RI* band light curves which are similar to our V band data and are consistent with significant cyclotron emission from the main accretion region.

There is a deep dip in soft energies during the bright phase (ϕ =0.84 in Figure 2). These dips are due to the ac-

	V347 Pav	GG Leo	EU UMa
Date	2002 Mar 16	2002 May 13	2002 Jun 12
EPIC MOS	Small Window thin 5980 sec	Small Window thin 7975 sec	Small Window thin 5792 sec
EPIC pn	Small Window thin 5053 sec	Small Window thin 7053 sec	Small Window thin 4870 sec
RGS	6453 sec	8448 sec	6265 sec
OM	Image/fast UVW1 1500 sec	Image/fast UVW1 2500 sec	Image/fast UVW1 1500 sec
OM	Image/fast UVW2 2000 sec	Image/fast UVW2 3000 sec	Image/fast UVW2 2000 sec
OM	Image/fast V 1500 sec	Image/fast V 1900 sec	Image/fast V 1500 sec
Mean V mag	16.8	17.1	18.2
Accretion state	High	High	High

Table 1. The log of *XMM-Newton* observations of V347 Pav, GG Leo & EU UMa. 'Thin' refers to the filter used. The exposure time in each detector is shown in seconds. The UVW1 filter has a coverage 2400–3400 Å and UVW2 1800–2400 Å.

cretion stream obscuring the accretion region on the white dwarf (*cf* Watson et al 1989). A similar dip is also seen in HST UV data of the polar QS Tel (de Martino et al 1998). Using the fit to the bright phase spectrum (which excludes the dip) shown in §4 as the reference model, we find that the neutral absorption must increase to $\sim 2 \times 10^{21}$ cm^{-2}to obtain the observed count rate in the 0.15–0.5keV energy band. This level of absorption has negligible affect on the count rate in the 1-10keV band.

To estimate the amount of absorption required to produce the decrease in the flux in the UVW2 band we used the Tübingen-Boulder inter-stellar medium absorption model. (Other absorption models included in `XSPEC` are not sensitive to absorption in the UV). This includes gas, grain and H_2 absorption and recent improvements in the photo-ionisation cross-sections: since we do not expect dust or H_2 molecules to be present in polars, we switch these parameters to zero. We find that the equivalent Hydrogen column density required to reduce the UVW2 flux by the observed amount is 7–8$\times 10^{21}$ cm^{-2}. This amount of absorption would have a noticeable affect on the 1–10keV flux, which we do not observe. The Tübingen-Boulder model is for a neutral absorber, and depending on the location of the absorber it will be irradiated to some degree. The fact that the result from this fit is inconsistent with the X-rays is indicative of such irradiation and/or other complex processes.

3.3 EU UMa

Like V347 Pav and GG Leo, EU UMa is principally a one pole system, showing a bright phase lasting ∼0.5 cycles (Figure 3). However, in contrast to V347 Pav and GG Leo, it shows very little flux above 1keV. This is similar to the *ROSAT* X-ray observations (Ramsay 1995). During the faint phase the source is weakly detected 0.012±0.004 ct/s in the EPIC pn detector.

Again in contrast to V347 Pav and GG Leo, the soft X-ray band shows prominent flaring activity. We performed a Discrete Fourier Transform on the soft X-ray light curve, but there was no evidence that the flare activity was modulated on a quasi-coherent period.

The OM data shows no large variations in the flux levels over the orbital period. The V band data cover the same phase interval as the sharp rise in X-ray flux. Unusually, there is no corresponding rise in the optical flux. Mittaz et al (1992) note that EU UMa shows an unusually high EUV/optical ratio. The UVW1 data were taken in the faint phase and show no significant variation, while there is some evidence that the UVW2 data reflect the decline from the bright phase.

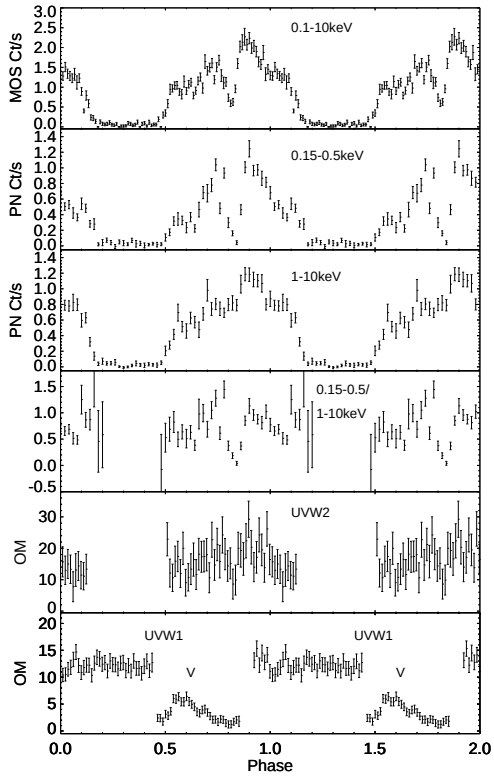

Figure 2. The binned X-ray and OM light curves of GG Leo. We fold the data on the orbital period of Burwitz et al (1998). The phasing is arbitrary. The 0.15–1.0keV data have been binned into 0.01 cycle bins while the 1.0–10.0keV band data and the OM data have been binned into 0.02 cycle bins. The units for the OM data are 10^{-16} ergs s^{-1} cm^{-2}Å^{-1}.

4 X-RAY SPECTRA

We extracted X-ray spectra from the bright phase of the 3 systems. In the case of GG Leo we excluded the phase interval where the prominent dip feature was seen. We extracted single and double events and used the response matrix epn_sw20_sdY9.rmf for the EPIC pn data together with

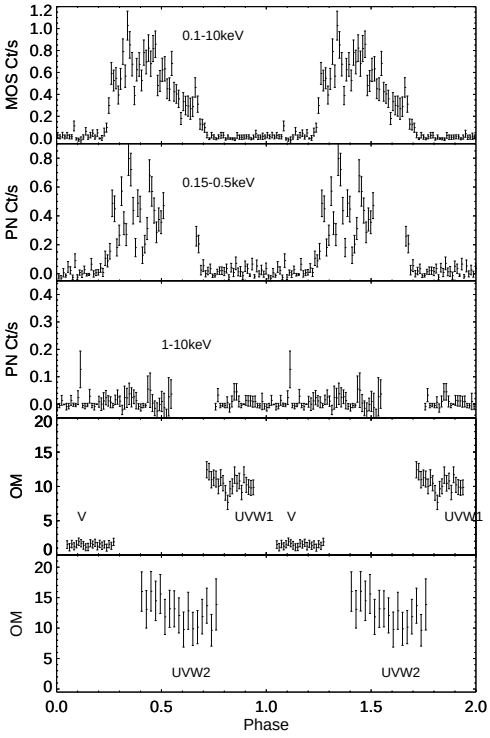

Figure 3. The X-ray and OM light curves of EU UMa. We fold the data on the orbital period of Howell et al (1995). We define the folding epoch (arbitrarily) at HJD=2452000. The 0.15–1.0keV data has been binned into 0.01 cycle bins and the 1.0–10.0keV data into 0.05 cycle bins. The UVW1 and V band OM data has been binned into 60 sec bins (=0.011 cycles) and the UVW2 into 120 sec bins (=0.022 cycles). The units for the OM data are 10^{-16} ergs s^{-1} cm^{-2}Å^{-1}.

an auxiliary file generated using the SAS task `arfgen`. We also extracted spectra using the EPIC MOS spectra. The results obtained using the MOS spectra were consistent with the pn spectra, but we show only the results using the pn data (for the sake of brevity) since these had the higher signal to noise ratio.

4.1 The model

We modelled the data using a simple neutral absorber and an emission model of the kind described by Cropper et al (1999). We have used this model in our previous studies of polars observed using *XMM-Newton* - we refer the reader to those papers for details (see §1). We fix the specific accretion rate at 1 g s^{-1} cm^{-2} and the ratio of cooling due to cyclotron to bremsstrahlung at the shock at 5. We also added a blackbody component and, if necessary, a neutral absorber with a partial covering fraction. We show in Table 2 the derived spectral parameters with the goodness of fits.

4.2 The spectral fits

We show the EPIC pn spectra in Figure 4 (V347 Pav), Figure 5 (GG Leo) and Figure 6 (EU UMa). As expected from the energy resolved light curves, both GG Leo and V347 Pav show strong hard X-ray components, while this is weak in EU UMa. We obtain good fits (Table 2) to the spectra

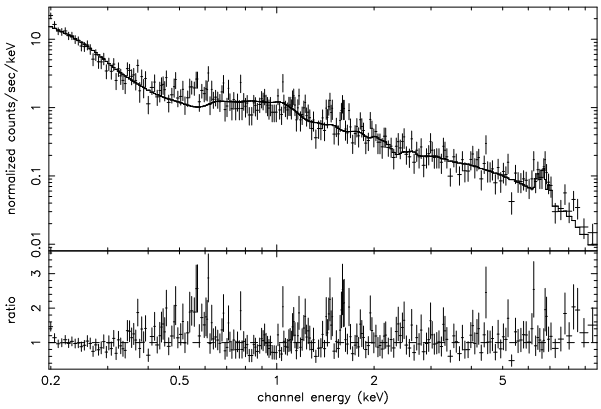

Figure 4. The bright phase EPIC pn spectra of V347 Pav. The best fit model is shown as a solid line.

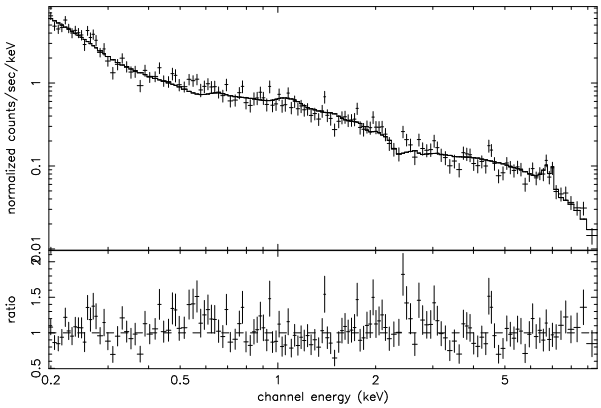

Figure 5. The bright phase EPIC pn spectra of GG Leo (the accretion stream dip interval has been excluded). The best fit model is shown as a solid line.

of EU UMa and V347 Pav, with significant residuals in GG Leo (χ^2_ν=1.40). In the case of GG Leo and V347 Pav we require the addition of a neutral absorber with partial covering to achieve good fits. In the case of V347 Pav (and to a lesser extent GG Leo) there are prominent residuals near 0.5–0.6keV and also 1.45 and 1.60keV. Our model includes line emission from collisionally ionised plasma but does not include emission from photo-ionised plasma, seen in sources such as X-ray binaries where there is a strong irradiating source. One prominent photo-ionised emission line is the OVII He-like triplet near 0.57 keV which may be the source of the residuals at these energies. Emission lines near 1.45keV and 1.60keV are Mg XII and Mg XI.

4.3 The energy balance

In Table 2 we show the luminosities of both the soft and hard X-ray components. We define the hard X-ray luminosity as $L_{X-hard,bol} = 4\pi \mathrm{Flux}_{X-hard,bol} d^2$ where $\mathrm{Flux}_{X-hard,bol}$ is the unabsorbed, bolometric flux from the hard X-ray component and d is the distance and the soft X-ray luminosity as $L_{soft,bol} = \pi \mathrm{Flux}_{soft,bol} \sec(\theta) d^2$. We refer the reader to Ramsay & Cropper (2003a) for further details.

We show in Table 2 the ratio $L_{bb,bol}/L_{X-hard,bol}$ for each source. These ratios do not include the geometrical cor-

Source	N_H (10^{20}) cm^{-2}	kT_{bb} (eV)	M_{wd} ($M_\odot$)	Blackbody Flux ($\times10^{-11}$)	X-hard Flux ($\times10^{-11}$)	$L_{bb,bol}$ ($\times10^{31}$)	$L_{X-hard,bol}$ ($\times10^{31}$)	$L_{bb,bol}/L_{X-hard,bol}$ ($\times10^{31}$)	χ^2_ν (dof)
EU UMa	$0.1^{+3.7}_{-0.1}$	20^{+3}_{-7}	$1.2^{+0.2}_{-0.1}$	$12.7^{+17600}_{-7.5}$	$0.06^{+0.02}_{-0.05}$	$3.8^{+5300}_{-2.3}$	$0.08^{+0.03}_{-0.06}$	$46.9^{+2780}_{-33.3}$	0.95 (28)
GG Leo	$0.0^{+0.6}$	38^{+4}_{-3}	1.13±0.03	$2.0^{+0.7}_{-0.2}$	$3.10^{+0.06}_{-0.13}$	$0.6^{+0.2}_{-0.1}$	$3.7^{+0.1}_{-0.2}$	$0.16^{+0.07}_{-0.02}$	1.40 (136)
	840^{+220}_{-160}, 0.65±0.02								
V347 Pav	$0.0^{+0.4}$	32±3	1.00±0.06	$6.4^{+2.2}_{-0.4}$	$2.21^{+0.08}_{-0.09}$	$1.9^{+0.6}_{-0.1}$	$2.7^{+0.1}_{-0.2}$	$0.70^{+0.3}_{-0.1}$	1.02 (237)
	$5.6^{+3.6}_{-1.6}$ 0.50±0.03								

Table 2. The fits to the X-ray data. The blackbody bolometric luminosity, $L_{bb,bol}$ and the X-ray luminosity from the shock, $L_{Xhard-bol}$, are defined in the text. The units of flux are ergs s^{-1} cm^{-2}and luminosity ergs s^{-1}: we assume a distance of 100 pc in each case. The metal abundance was fixed at solar. The errors are quoted at the 90 percent confidence level.

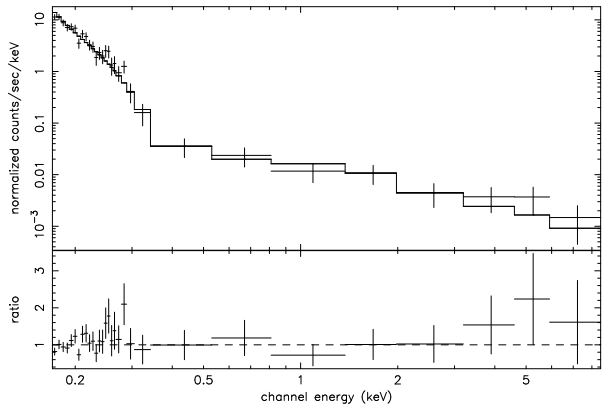

Figure 6. The bright phase EPIC pn spectra of EU UMa. The best fit model is shown as a solid line.

rection term sec(θ) for the blackbody component. For EU UMa and GG Leo we do not know the viewing angle to the accretion region. A mean viewing angle of 50° and 80° implies a correction of 1.55 and 5.8 respectively. Even without a geometrical correction, EU UMa shows one of the highest soft/hard ratios ever observed in a polar. Its X-ray emission is likely to be dominated by the accretion of dense blobs which impact the photosphere of the white dwarf directly without forming a shock (Kuijpers & Pringle 1982). In contrast GG Leo shows an energy balance consistent with the standard accretion model (which predicts a ratio ∼0.5) for a high mean viewing angle. For V347 Pav, Potter, Cropper & Hakala (2000) estimate an inclination of 64–72°, a dipole offset less than 8° and that the main accretion pole is located near the magnetic equator. This implies the viewing angle is $\sim 30-40°$ and the geometrical correction is 1.15–1.30. Therefore V347 Pav shows a small excess over the standard shock model, but this excess is likely to disappear were the contribution from cyclotron emission to be included. We discuss the energy balance of our full *XMM-Newton* sample of polars in Ramsay & Cropper (2003c), although a preliminary view is given in Ramsay & Cropper (2003b).

4.4 The white dwarf mass

We can infer the mass of the white dwarf from our model fitting, assuming a mass-radius relationship for the white dwarf. As usual we assume the Nauenberg (1972) relationship. From fitting the 0.2–10keV spectra we estimate a white dwarf mass of 1.0–1.1$M_\odot$for all 3 polars in this study.

For sources relatively strong in hard X-rays, it is also possible to restrict the energy range so that the fitted range is above the main absorption edges (most of which are below ∼2keV). We fitted the spectra of V347 Pav and GG Leo in the energy range 3–10keV. We stepped through a range of white dwarf masses and metal abundances. The fits to these spectra are shown in Table 3. For V347 Pav we find the fits are very similar for a white dwarf mass between 0.6–1.0$M_\odot$. For GG Leo a white dwarf of mass 0.6$M_\odot$gives significantly poorer fits compared to a 0.8 or 1.0$M_\odot$white dwarf.

We then used the optimal fits to these models and fitted them over the extended energy range 0.2-10.0keV. We kept the shock emission model fixed and added a blackbody and partial covering model (which were allowed to vary). The results to the fits are also shown in Table 3. We find that for V347 Pav, the resulting fit is still reasonably good (χ^2_ν∼1.1) although the best fit model (Table 2) is formally a better fit at the >99% confidence level. In the case of GG Leo, for a white dwarf mass of 1.0$M_\odot$and a metal abundance of 0.5 solar, the fit is very similar to that found before. Lower masses (of both solar and 0.5 solar metallicities) gave significantly poorer fits.

Our technique of determining masses has been controversial in that for many systems our X-ray fitting method predicts rather heavy masses (1$M_\odot$or more) (eg Schwope et al 2002). The main criticism has been that for energies less than ∼2keV, the uncertainties in the absorption limit the accuracy that the mass can be determined. We have shown here that by excluding energies less than 3keV, the masses for GG Leo and V347 Pav were lower than when we used the full spectral range. However, these fits were poorer at the formal level. This may be due to the absorption being much more complex than the relatively simple treatment assumed here. We accept that for systems which have sufficiently strong hard X-ray components to achieve the necessary signal to noise ratio it is desirable to use energies above 3keV to fix this component. However, even when we do this in the case of GG Leo the best fit mass is still ∼1$M_\odot$.

We noted in §4.2 the presence of residuals in the spectral fits near 0.57keV which maybe due to our emission model not including photo-ionised lines. Emission from this triplet is seen in the intermediate polar EX Hya (Cropper et al 2002) which has a white dwarf mass of 0.5$M_\odot$. If the ionising source was stronger then this would result in stronger

Source	3–10keV			0.2–10keV		
	M	Z ($\odot$)	χ^2(dof)	M	Z ($\odot$)	χ^2(dof)
V347	1.0	1.0	54.3 (56)	1.0	1.0	295.2 (242)
Pav	0.8	1.0	55.4 (56)	0.8	1.0	268.6 (242)
	0.6	1.0	61.6 (56)	0.6	1.0	285.6 (242)
	1.0	0.5	56.6 (56)	1.0	0.5	271.1 (242)
	0.8	0.5	56.0 (56)	0.8	0.5	273.5 (242)
	0.6	0.5	57.7 (56)	0.6	0.5	290.4 (242)
GG	1.0	1.0	38.2 (35)	1.0	1.0	221.4 (141)
Leo	0.8	1.0	47.6 (35)	0.8	1.0	266.5 (141)
	0.6	1.0	72.1 (35)	0.6	1.0	328.5 (141)
	1.0	0.5	37.8 (35)	1.0	0.5	203.0 (141)
	0.8	0.5	40.3 (35)	0.8	0.5	234.1 (141)
	0.6	0.5	49.0 (35)	0.6	0.5	291.9 (141)

Table 3. We fitted the spectra in the energy range 3–10keV using an absorbed stratified accretion column model and stepped through a range of white dwarf masses and metal abundance. We then fixed these emission models and fitted in the extended energy range 0.2–10.0keV after adding a blackbody and partial covering component. In comparison when we allowed the parameters of the stratified emission to vary the fits were χ^2=241.7 (237) and χ^2=190.4 (136) for V347 Pav and GG Leo respectively. For five extra parameters the difference in $\chi^2$is 9.24 and 11.3 at the 90% and 99% confidence levels.

photo-ionised lines. If the white dwarf was more massive then the ionising source would be stronger and result in more prominent emission near 0.57keV. This is consistent with our, rather heavy, mass estimates.

4.5 The UV fluxes

We use the best fit models in Table 2 to predict the flux in the OM UV filters. The flux from the post-shock accretion flow falls well below the observed UV flux in all three systems. This indicates that the emission from the unheated photosphere of the white dwarf must dominate in the UV.

We can estimate the temperature for our objects based on their UV filter flux ratios. Here we use the mean flux taken from those orbital phases where there were data from both filters. We use model white dwarf Hydrogen atmosphere models of covering a range of temperature which were kindly supplied by Detlev Koester. We take the neutral absorption reported from our fits to the X-ray data (Table 2) and convert this to optical extinction using the relationship of Predehl & Schmitt (1995). Assuming the absorption derived from the X-ray fits are appropriate we find that the temperature of the white dwarf us is <10200K for V347 Pav and 9200–10400K and 9200-11500K for GG Leo and EU UMa respectively. This is similar to the temperatures determined for the unheated white dwarf by Gänsicke (1998). (The temperatures determined using a simple blackbody approximation are similar being ∼3000 K hotter than that derived using white dwarf atmosphere models).

Using the white dwarf atmosphere models of Koester we can set the normalisation so that it gives the measured flux in the UV filters (this is in addition to the model used to fit the X-ray spectra). If we assume a white dwarf of certain radius (based on the derived masses in §4.4) we can obtain a distance estimate. Naturally since the luminosity of the white dwarf is proportional to T^4 and the calibration of the UV filters is reliable to ∼5 percent, we should approach these distances with due caution. With this in mind, we estimate distances of ∼40-50pc, 50-70pc and 60-80pc for V347 Pav, GG Leo and EU UMa respectively.

5 ACKNOWLEDGMENTS

We thank Detlev Koester for kindly supplying his white dwarf model atmosphere spectra. This paper is based on observations obtained with XMM-Newton, an ESA science mission with instruments and contributions directly funded by ESA Member States and the USA (NASA).

REFERENCES

Bailey J., Ferrario L., Wickramasinghe D. T., Buckley D., Hough J., 1995, MNRAS, 272, 579
Burwitz V. et al, 1998, A&A, 331, 262
Cropper M., Wu K., Ramsay G., Kocabiyik A., 1999, MNRAS, 306, 684
Cropper M., Ramsay G., Hellier C., Mukai K., Mauche C., Pandel D., 2002, Phil Trans R Soc Lond A., 360, 1951
de Martino D., Mouchet M., Rosen S. R., Gänsicke B., 1998, A&A, 329, 571
Gänsicke B., 1998, In Proc 13th N. American workshop on CVs, ASP Conf Series, 137, 88
Howell S., Sirk M., Malina R., Mittaz J. P. D., Mason K. O., 1995, ApJ, 439, 99
King A. R., Lasota J. P., 1979, MNRAS, 188, 653
Kuijpers J., Pringle J. E., 1982, A&A, 114, L4
Lamb D. Q., Masters A. R., 1979, ApJ, 234, 117
Mason K. O., et al 2001, A&A, 365, L36
Mittaz J. P. D., Rosen S. R., Mason K. O., Howell S. B., 1992, MNRAS, 258, 277
Nauenberg M., 1972, ApJ, 175, 417
O'Donoghue D., Mason K. O., Chen A., Hassall B. J. M., Watson M. G., 1993, MNRAS, 265, 545
Pounds K. A. et al. 1993, MNRAS, 260, 77
Potter S., Cropper M., Hakala P., 2000, MNRAS, 315, 423
Predehl P., Schmitt J. H. M. M., 1995, A&A 293 889
Ramsay G., Mason K. O., Cropper M., Watson M. G., Clayton K. L., 1994, MNRAS, 270, 692
Ramsay G., 1995, PhD Thesis, Univ London
Ramsay G., Cropper M., Wu K., Potter S., 1996, MNRAS, 282, 726
Ramsay G., Cropper M., Cordova F., Mason K., Much R., Pandel D., Shirey R., 2001, MNRAS, 326, L27
Ramsay G., Cropper M., 2002a, MNRAS, 334, 805
Ramsay G., Cropper M., 2002b, MNRAS, 335, 918
Ramsay G., Cropper M., 2003a, MNRAS, 338, 219
Ramsay G., Cropper M., 2003b, In Proc Cape Town Workshop on mCVs, astro-ph/0301609
Ramsay G., Cropper M., 2003c, submitted, MNRAS
Schwope A. D., Hambaryan V., Schwarz R., Kanbach G., Gänsicke B. T., 2002, A&A, 392, 541
Watson M. G., King A. R., Jones M. H., Motch C., 1989, 237, 299
Warner B., 1995, Cataclysmic variable stars, Cambridge Univ. Press, Cambridge